five variational equations of (5) form a complete set of linear equations with periodic coefficients to which Floquet theory[3] may be applied to study stability in the small of the attitude motion of the satellite symmetry axis.

The system parameter space is of dimension four with components K_1, K_2, ρ, and ϵ. In this study the parameter K_1 was held at the constant value 0.20 and the remaining parameters were varied over the ranges $0 < K_2 < 0.30$, $0 < \rho < 200$, and $0 < \epsilon < 0.25$. The results of the Floquet analysis for four planes associated with constant values of $\epsilon = 0.01, 0.05, 0.10$, and 0.20 are shown in Figs. 1, 2, 3, and 4 respectively. The influence of orbit eccentricity in this study is qualitatively similar to the results obtained by Kane and Barba. For a circular orbit, $\epsilon = 0$, there are two unstable bands in the (ρ,K_2) plane, as was determined by Shippy and Robe. As ϵ is increased, these bands labeled I and II, gradually widen and two additional unstable regions, labeled III and IV, appear where the motion was previously stable for a circular orbit. Figures 1, 2, 3, and 4 illustrate that the unstable regions (I and III) and (II and IV) tend to merge with increasing ϵ. Finally, at $\epsilon \simeq 0.25$, the entire (ρ,K_2) plane, with the exception of a very narrow band separating the (I,III) and (II,IV) regions, corresponds to unstable attitude motion.

References

[1] Kane, T. R. and Barba, P. M., "Attitude Stability of a Spinning Satellite in an Elliptic Orbit," *Journal of Applied Mechanics*, Vol. 33, No. 2, June 1966, pp. 402–405.

[2] Shippy, D. J. and Robe, T. R., "Effect of a Rotor on the Attitude Stability of a Non-Spinning Symmetrical Satellite," Fourth Southeastern Conference on Theoretical and Applied Mechanics, New Orleans, La., Feb. 29–March 1, 1968.

[3] Coddington, E. L. and Levinson, N., *Theory of Ordinary Differential Equations*, McGraw-Hill, New York, 1955, pp. 78–81.

Collapse Loads of Partially Loaded Clamped Shallow Spherical Caps

C. E. Dumesnil*
Vought Aeronautics Division, LTV Aerospace Corporation, Dallas, Texas

AND

G. E. Nevill Jr.†
University of Florida, Gainesville, Fla.

In 1968, Lee and Onat[1] gave an exact solution for collapse loads of uniformly loaded axially symmetric spherical shells of a rigid-plastic material which obeys the Tresca yield condition and flow law. This Note extends their work to caps with a uniform axially symmetric partial load. The nomenclature is that of Ref. 1 except that φ replaces S.

Stress Field

The equations of equilibrium for the cap, from Ref. 1 are

$$\begin{aligned} n'_\varphi &= [n_\theta - n_\varphi - (n_\varphi + p)\tan^2\varphi]\cot\varphi \\ m'_\varphi &= [m_\theta - m_\varphi - (1/k)(n_\varphi + p)\tan^2\varphi]\cot\varphi \end{aligned} \tag{1}$$

Received June 16, 1969; revision received October 2, 1969. The authors express their appreciation to NASA for support of this research under Grant NGR 10-005-036.

* Engineering Specialist.

† Professor, Department of Engineering Science and Mechanics, College of Engineering.

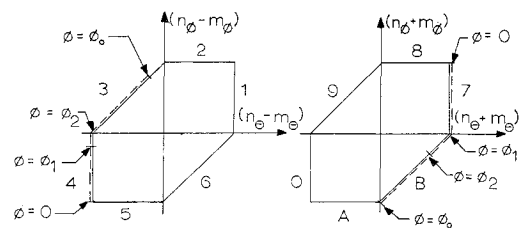

Fig. 1 Yield surface for clamped cap.

for the loaded region of the cap, $0 \le \varphi \le \varphi_L$, and

$$\begin{aligned} n'_\varphi &= \left[n_\theta - n_\varphi - n_\varphi\tan^2\varphi - p\,\frac{\sin^2\varphi_L}{\cos^2\varphi}\right]\cot\varphi \\ m'_\varphi &= \left[m_\theta - m_\varphi - \frac{1}{k}\,n_\varphi\tan^2\varphi - \frac{1}{k}\,p\,\frac{\sin^2\varphi_L}{\cos^2\varphi}\right]\cot\varphi \end{aligned} \tag{2}$$

for the unloaded region of the cap, $\varphi_L \le \varphi \le \varphi_0$.

The Tresca sandwich yield surface is represented in Fig. 1. The analysis begins by choosing a collapse pressure p^* and determining an appropriate stress state at the center of the shell. Following Ref. 1, the starting point on the yield surface is chosen as the intersection of faces 45 and 78. The stress point then moves along face 47 on which $n_\theta = 0$ and $m_\theta = 1$. Utilizing these conditions and the initial conditions $n_\varphi = 0, m_\varphi = 0$ at $\varphi = 0$, Eqs. (1) are solved to obtain

$$n_\varphi = -p^*(1 - \varphi\cot\varphi),\ m_\varphi = 1 - (1/k)p^*(1 - \varphi\cot\varphi) \tag{3}$$

for the region $0 \le \varphi \le \varphi_1$. The stress point motion on 47 is interrupted when 7B is reached, where $n_\varphi + m_\varphi = 0$. This condition, with Eqs. (3), is used to determine φ_1.

If plastic deformation is to occur everywhere, further motion of the stress point must be along 4B, where the conditions $m_\theta = 1 + n_\theta$ and $n_\varphi = \frac{1}{2}(n_\varphi + m_\varphi)$ hold. These conditions, combined with Eqs. (1), yield the second-order differential equation

$$n''_\varphi + n'_\varphi\left[\frac{2}{\sin\varphi\cos\varphi}\right] + n_\varphi\left[2\sec^2\varphi + \frac{1}{2}\left(\frac{1+k}{k}\right)\right] = \frac{1}{2}\cot^2\varphi - p^*\left[2\sec^2\varphi + \frac{1}{2}\left(\frac{1+k}{k}\right)\right] \tag{4}$$

This equation was solved numerically using a fourth-order Runge-Kutta stepping method,[2] with initial conditions on n_φ at φ_1 obtained from Eq. (3). The motion on 4B continues to corner 34. This point, φ_2, is determined by the condition $n_\varphi - m_\varphi = 0$. The stress point then moves on 3B, where $n_\theta = n_\varphi$ and $m_\theta = 1 + m_\varphi$. This condition, with Eqs. (1), allows the solution, in the region $\varphi_2 \le \varphi \le \varphi_L$,

$$\begin{aligned} n_\varphi &= C_1\cos\varphi - p^* \\ m_\varphi &= \ln(\sin\varphi) + (1/k)C_1\cos\varphi + C_2 \end{aligned} \tag{5}$$

C_1 and C_2 are determined by requiring continuity at φ_2.

For $\varphi \ge \varphi_L$, the cap is unloaded and further motion on 3B is controlled by Eqs. (2). With the requirements of 3B, (2) yields

$$\begin{aligned} n_\varphi &= C_3\cos\varphi - p^*\sin^2\varphi_L[1 + \cos\varphi\ln(\tan\varphi/2)] \\ m_\varphi &= \ln(\sin\varphi) + (1/k)C_3\cos\varphi - (1/k)p^*\sin^2\varphi_L \times \\ &\qquad \cos\varphi\ln\{\tan(\varphi/2)\} + C_4 \end{aligned} \tag{6}$$

C_3 and C_4 are determined from continuity conditions at $\varphi = \varphi_L$. The stress point continues on 3B to the corner AB where $-n_\varphi - m_\varphi = 1$. The angle $\varphi = \varphi_0$ where this occurs is a possible location for the clamped edge of the cap. Thus, a statically admissible stress field has been obtained and the chosen p^* is a lower bound on the collapse pressure for a shell with half opening angle φ_0.

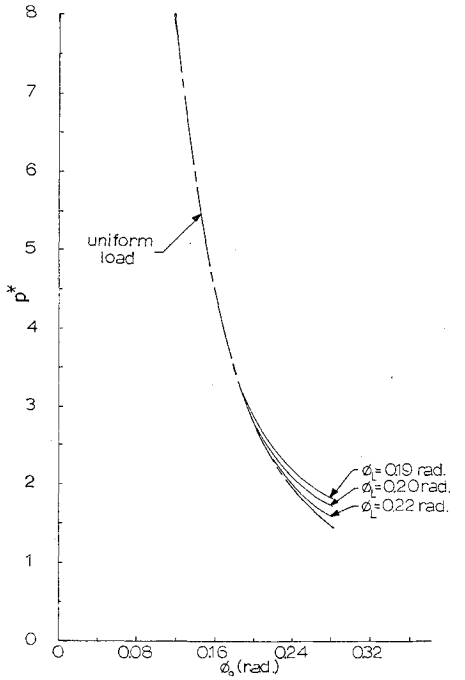

Fig. 2 Load carrying capacity for clamped shells with $k = 1/50$.

Velocity Field

Eliminating the displacement components from the generalized strain rate-velocity relations in Ref. 1 yields the compatibility relations

$$\begin{aligned} \epsilon'_\theta &= [\epsilon_\varphi - \epsilon_\theta + (1/k)\varkappa_0 \tan^2\varphi] \cot\varphi \\ \varkappa'_\theta &= (\varkappa_\varphi - \varkappa_\theta \sec^2\varphi) \cot\varphi \end{aligned} \tag{7}$$

In Ref. 1, it is shown that the clamped edge boundary conditions are $\lambda_1 = 0$ and $\lambda_2 = \cot\varphi_0$ (where λ_1 and λ_2 are the non-negative constants in the flow rule) and the λ's must be continuous in passing from one plastic regime to another. Following Ref. 1, the velocity solution begins at the clamped edge; since there is a sign requirement on the λ's, equations involving only λ_1 and λ_2 are used. The flow rule for faces 3B, as given in Ref. 1, combined with Eq. (7), yields

$$\begin{aligned} d\lambda_1/d\varphi &= \tfrac{1}{2}\{[-4\cot\varphi - (1+\alpha)\tan\varphi]\lambda_1 - \\ &\qquad [(1+\alpha)\tan\varphi]\lambda_2\} \\ d\lambda_2/d\varphi &= \tfrac{1}{2}\{-[(1-\alpha)\tan\varphi]\lambda_1 - [4\cot\varphi + \\ &\qquad (1-\alpha)\tan\varphi]\lambda_2\} \end{aligned} \tag{8}$$

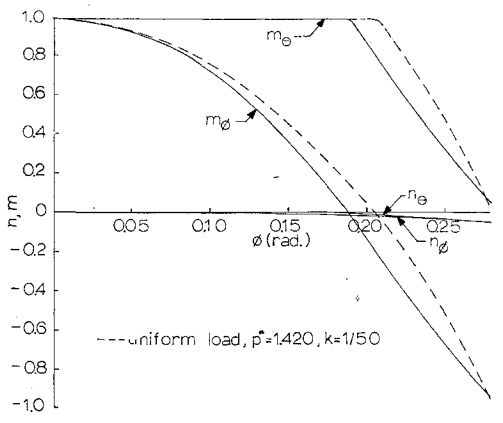

Fig. 3 Stress distribution for $p^* = 1.715$, $k = 1/50$, $\varphi_L = 0.20$ rad.

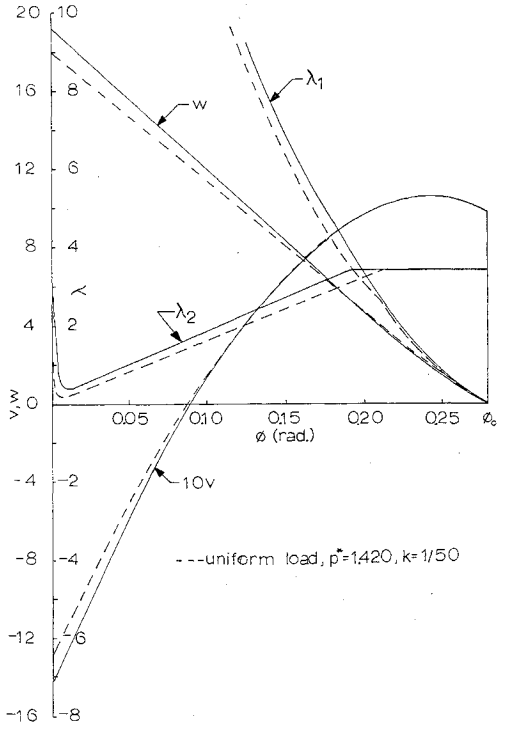

Fig. 4 Velocity distribution for $p^* = 1.715$, $k = 1/50$, $\varphi_L = 0.20$ rad.

where $\alpha = 1/k$. Similarly for faces 4B

$$\begin{aligned} d\lambda_1/d\varphi &= \tfrac{1}{2}\{-[2\cot\varphi + (1+\alpha)\tan\varphi]\lambda_1 - \\ &\qquad [(1+\alpha)\tan\varphi]\lambda_2\} \\ d\lambda_2/d\varphi &= \tfrac{1}{2}\{-[(1-\alpha)\tan\varphi]\lambda_1 - [2\cot\varphi + \\ &\qquad (1-\alpha)\tan\varphi]\lambda_2\} \end{aligned} \tag{9}$$

and for faces 47

$$\begin{aligned} d\lambda_1/d\varphi &= \tfrac{1}{2}\{-[2\cot\varphi - (1+\alpha)\tan\varphi]\lambda_1 - \\ &\qquad [(1+\alpha)\tan\varphi]\lambda_2\} \\ d\lambda_2/d\varphi &= \tfrac{1}{2}\{[(\alpha-1)\tan\varphi]\lambda_1 - [2\cot\varphi - \\ &\qquad (\alpha-1)\tan\varphi]\lambda_2\} \end{aligned} \tag{10}$$

The velocity field was then obtained by numerical integration of these equations.

A final check was made to insure that λ's were non-negative. With a kinematically admissible velocity field and associated statically admissible stress field, a complete solution to the problem has been obtained.

Results and Discussion

The collapse pressure p^* is shown in Fig. 2 as a function of cap angle φ_0 and load angle φ_L. Figures 3 and 4 show the resulting stress and velocity distributions for $\varphi_L = 0.20$ rad compared with those obtained for the uniformly loaded cap. It is seen that a shallow shell solution similar to that obtained in Ref. 1 is valid for the partially loaded cap for angles φ_0 up to 0.28 rad and for values $\varphi_L = 0.19$ rad or larger. Within these ranges, collapse pressure and stress and velocity distributions remain close to those of the uniformly loaded cap.

In order to extend the solution for partial loading to larger angles φ_0, it is expected that deep shell relations would have to be used and that the deep shell solution of Lee and Onat, Ref. 1, could be used for guidance. For angles $\varphi_L \leq 0.19$ rad, it is expected that significantly different stress and velocity distributions would be obtained. Since Lee and Onat found distributions with jumps present for deeper shells and since the partially loaded shell involves a discontinuity in loading, it is expected that discontinuous solutions might be

found for values of $\varphi_L \leq 0.19$ rad. Up to the present, it has not been possible to find such solutions.

References

[1] Lee, L. C. and Onat, E. T., "Analysis of Plastic Spherical Shells," *Engineering Plasticity*, edited by J. Heyman and F. A. Leckie, Cambridge Univ. Press, pp. 413–442, 1968.

[2] James, M. L., Smith, G. M., and Walford, J. C., *Applied Numerical Methods for Digital Computation with FORTRAN*, International Textbook, Scranton, Pa., 1967.

Prestressing in Structural Synthesis

LAWRENCE D. HOFMEISTER*
TRW Systems, Redondo Beach, Calif.
AND
LEWIS P. FELTON†
University of California, Los Angeles, Calif.

Introduction

PRESTRESSING is a recognized device for improving structural efficiency. The most widespread applications are found in concrete construction, where precompression is introduced into structures in order to limit or eliminate tenile stresses and consequent brittle failure. The immediate effect of such prestressing is usually a reduction in weight and/or deflection compared to that of nonprestressed structures.

Application of prestressing to structures composed of other than brittle materials occurs relatively infrequently, even in aerospace applications where the potential enhancement of high-performance structures could prove significant. This situation is probably attributable both to the lack of a comprehensive approach to optimization of prestressed structures and to fabrication difficulties.

This Note attempts to clarify the first area by describing a general method for including prestressing in the minimum-weight design of statically indeterminate structures. The design problem is formulated as a constrained minimization problem, and the magnitude of the prestress, as well as the usual parameters, are considered as variables which must be selected optimally.

Synthesis

It has been shown[1] that the minimum-weight structural design problem can be cast in the form of a mathematical programing problem as follows:

$$\text{Minimize } f(\mathbf{X}) \text{ over } \mathbf{X}$$
$$\text{such that } g_k(\mathbf{X}) \geq 0 \text{ for all } k \tag{1}$$

where $\mathbf{X} = \{x_1\, x_2 \ldots x_n\}$ is a vector of design variables, $f(\mathbf{X})$ is the objective function, and the $g_k(\mathbf{X})$ are constraint functions. The design variables may be, for example, cross-sectional areas of members in truss design, and so on. The objective function is taken as the total weight of the structural system, and the constraints limit structural behavior. For example, the constraints may specify that member stresses do not exceed limiting values, or that deflections remain within specified bounds. Equations (1) can be solved numerically by searching systematically over the acceptable values of $\mathbf{X}$ [i.e., those $\mathbf{X}$ for which $g_k(\mathbf{X}) \geq 0$] for the minimum of the objective function. In general, $f(\mathbf{X})$ and the $g_k(\mathbf{X})$ are nonlinear functions of the x_i.

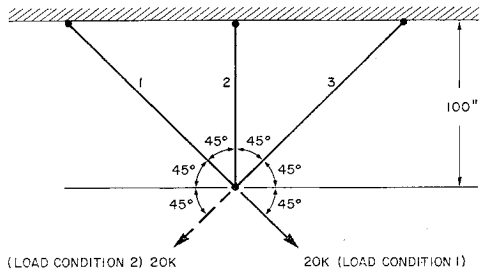

Fig. 1 Truss design example.

Consider now that prestressing can be introduced either by the use of high-strength tension cables as in concrete structures, or alternately could be induced by an initial lack of fit of the structural members if the system is indeterminate. In either case let the vector of original design variables $\mathbf{X}$ be augmented by $x_{n+1}, \ldots, \ldots, x_m$, where the additional variables represent unknown quantities associated with the prestressing. For example, with cable prestressing, the new variables will represent initial values of precompression for each component of the system. If the system is initially stressed by lack of fit, the additional design variables may be taken as the changes in length of each member necessary to achieve the prestress. The augmented vector $\{x_1, \ldots, x_{n+1}, \ldots, x_m\}$ will be denoted by $\hat{\mathbf{X}}$. It should be noted that the initially prestressed structure must satisfy all conditions of displacement compatibility.

If it is assumed that the prestressing mechanism does not contribute significantly to the total structural weight, then the objective function remains dependent only on $\mathbf{X}$ rather than $\hat{\mathbf{X}}$. The effect of the prestressing on the design problem then enters by way of the constraint equations. For example, if a structural analysis reveals that the stress in member i under load condition j is $\sigma_{ij}(\mathbf{X})$, then the stress constraints can take the normalized form

$$g_k(\mathbf{X}) = [\sigma_y - \sigma_{ij}(\mathbf{X})]/\sigma_y \geq 0 \tag{2}$$

where σ_y may be a yield stress of the material or other allowable stress limit. For a linearily responding structural system, the prestressing modifies the stress distribution to $[\sigma_{ij}(\mathbf{X}) + \hat{\sigma}_i(\hat{\mathbf{X}})]$ where the $\hat{\sigma}_i(\hat{\mathbf{X}})$ is caused by the prestress. (Since this additional stress is a constant for all loading conditions, the second subscript has been dropped.) The constraints on stress behavior now become

$$\hat{g}_k(\hat{\mathbf{X}}) = [\sigma_y - \sigma_{ij}(\mathbf{X}) - \hat{\sigma}_i(\hat{\mathbf{X}})]/\sigma_y \geq 0 \tag{3}$$

In addition to the modified stress constraints, Eq. (3), the structure must now withstand the initial stresses induced by prestress before any load is applied. Thus, supplementary stress constraints of the form

$$\hat{g}_p(\hat{\mathbf{X}}) = [\hat{\sigma}_y - \hat{\sigma}_i(\hat{\mathbf{X}})]/\hat{\sigma}_y \geq 0 \tag{4}$$

are necessary. Here $\hat{\sigma}_y$ may or may not equal σ_y. Deflection or other behavioral constraints can be modified in a similar manner.

The new mathematical programing problem can now be stated in a general form as

$$\min_{\hat{\mathbf{X}}} f(\mathbf{X}) \text{ such that } \hat{g}_k(\hat{\mathbf{X}}) \geq 0 \text{ for all } k \tag{5}$$

Examples

In order to illustrate the preceding method, the planar truss of Fig. 1 will be considered. This example was first

Received September 25, 1969. This research was partially supported by Grant NsG-423 from NASA to the late F. R. Shanley, Professor of Engineering, University of California, Los Angeles, Calif.

* Member of the Technical Staff. Formerly Postgraduate Research Engineer, University of California, Los Angeles, Calif.

† Assistant Professor of Engineering. Member AIAA.